

## Temporal variations of accumulation and temperature during the past two centuries from Belukha ice core, Siberian Altai

Keith Henderson,<sup>1</sup> Andreas Laube,<sup>1</sup> Heinz W. Gäggeler,<sup>1,2</sup> Susanne Olivier,<sup>1,2</sup> Tatyana Papina,<sup>3</sup> and Margit Schwikowski<sup>1</sup>

Received 29 January 2005; revised 5 October 2005; accepted 24 October 2005; published 9 February 2006.

[1] The temporal variation of accumulation and temperature in the Siberian Altai were investigated using a 86 m long ice core from Belukha glacier (49°48'26"N, 86°34'43"E, 4062 m a.s.l.), covering the time period 1816 to 2001. As temperature-sensitive parameters the melt percent profiles and the stable oxygen isotopes ( $\delta^{18}\text{O}$ ) were evaluated, representing summer season and March to November temperatures, respectively. The accumulation record showed no long-term trend and only minor deviations of limited duration from the accumulation average of 0.5 m water equivalent/y (weq./y) were observed. In contrast, the two temperature proxies indicate a strong warming trend in the order of  $1.6 \pm 0.4^\circ\text{C}$  and  $1.7 \pm 1.1^\circ\text{C}$  over the last century, inferred from melt percentages and the  $\delta^{18}\text{O}$  record, respectively, and  $2.5 \pm 1.7^\circ\text{C}$  since the mid-19th century, inferred from the  $\delta^{18}\text{O}$  record. This reflects an amplified regional climate response following the Little Ice Age (LIA) as compared to the Northern Hemisphere average, most probably caused by the strong continentality of the Siberian Altai region. The sudden onset of large melt features since 1988 indicates that the upper reaches of Belukha glacier are experiencing a change from the recrystallization to the cold-infiltration zone that now allows for multiannual percolation of meltwater, implying that the conservation of accumulation and geochemical properties, including those providing temperature proxies, is currently endangered.

**Citation:** Henderson, K., A. Laube, H. W. Gäggeler, S. Olivier, T. Papina, and M. Schwikowski (2006), Temporal variations of accumulation and temperature during the past two centuries from Belukha ice core, Siberian Altai, *J. Geophys. Res.*, *111*, D03104, doi:10.1029/2005JD005819.

### 1. Introduction

[2] Ice cores provide excellent archives of paleoenvironmental data from glaciated regions worldwide, each location commonly offering a unique picture of climate change over a variety of time windows, and representing regional variability that aids in reconstructing global-scale amplitudes and patterns of change [Cecil *et al.*, 2004]. Central Asia is a region with numerous opportunities for ice core studies, including the Himalaya, Tien Shan, Kunlun, Pamir, Qilian Shan, and Altai mountain ranges. This region is complex and meteorology is variable because of the weakening influence of the Asia-Pacific monsoon system across the Tibetan Plateau north toward the midlatitudes. The Altai Mountains (47–53°N, 84–92°E) define a rugged terrain that comprises the westernmost extent of Mongolia, and the common border regions of northern China, eastern Kazakhstan, and southwest Siberia. Approximately 1500 glaciers covering 900 km<sup>2</sup>

exist here, primarily on the central Altai Ukok Plateau and the Chuya and Katun ranges to the north and northwest, respectively. Local equilibrium line altitudes (ELA), the altitudes separating the accumulation and ablation zones on a glacier, rise from 2600 m in the northwest to 3800 m in the southeast, mainly because of precipitation (“rain-shadowing”) effects [Klinge *et al.*, 2003]. A strong, persistent retreat of outlet glaciers in the northeast Altai region has been observed over the last century, up to nearly 1 km and 2 km for the Maliy Aktru and Sofiyskiy glaciers (Chuya range), respectively [Pattyn *et al.*, 2003; Dyurgerov and Meier, 2000].

[3] The climatology of the Altai region is dominated by the regular wintertime development of the Siberian High, that leads to widespread extreme cold and dry conditions over much of central Siberia. Partly because of the regional peculiarities of the topography between the Altai and Lake Baikal to the east, the stable, stratified winter air mass establishes a persistent and deep inversion layer commonly 2 km in thickness, but often extending to reach even the higher land elevations of ~4 km [Lydolph, 1977]. As a result of the high continentality and the prevailing Siberian High in wintertime, seasonal temperature and precipitation cycles in the region are normally extreme. Summertime circulation brings sufficient moisture southward from the Kara Sea region, Russian Arctic

<sup>1</sup>Paul Scherrer Institute, Villigen PSI, Switzerland.

<sup>2</sup>Also at Department of Chemistry and Biochemistry, University of Bern, Bern, Switzerland.

<sup>3</sup>Institute for Water and Environmental Problems, Barnaul, Russia.



**Figure 1.** Map showing the location of Belukha glacier, the Tarvagatay Pass, and the Dundu glacier.

[Wedeland and Bryson, 1981] and allows for significant snowfall amounts on the Altai peaks ( $\sim 100$  mm weq./mo.). Locally, glacier extent studies show that moisture comes additionally from the southeast into specifically the northwest Altai (Katun). Snow lines, on the other hand, seem to respond primarily to the predominant northerly storm tracks ( $\sim 200$  m ELA rise from north-to-south aspect) [Klinge *et al.*, 2003].

[4] An important issue in ice core research continues to be the calibration of stable isotopes as a proxy for atmospheric temperatures, especially when taking into account the changes in the sources, circulation patterns, and seasonal distribution of precipitation. The linear relationship determined for mid- and high-latitude regions from simultaneous surface temperature ( $T_{sfc}$ ) and stable isotopic measurements on collected precipitation falls, in some cases, to provide the means for calibrating the scale of variation over longer time windows [Cuffey *et al.*,

1995; Jouzel *et al.*, 2003]. Because such biases are potentially caused by in-tandem changes to both the ambient temperatures and the seasonal distribution of snowfall, the issue of calibration becomes particularly important for a study area with high seasonal precipitation variability such as the Altai.

[5] Belukha, the highest mountain of the Altai (peak elevation 4506 m a.s.l., Figure 1), lies within the Katun range (ELA  $\sim 2800$  m) and supports a high, low-grade glaciated col between two summits. Following reconnaissance studies completed in 2000, deep drilling was accomplished on the Belukha saddle in 2001 including one core to bedrock. In a companion paper the temporal variations of mineral dust, biogenic tracers and anthropogenic species for the period 1815 to 2001 are presented [Olivier *et al.*, 2006]. Here, we investigate a pair of temperature-sensitive parameters ( $\delta^{18}\text{O}$ , melt percent) from Belukha ice core over the same time period to illustrate the patterns of warming in the

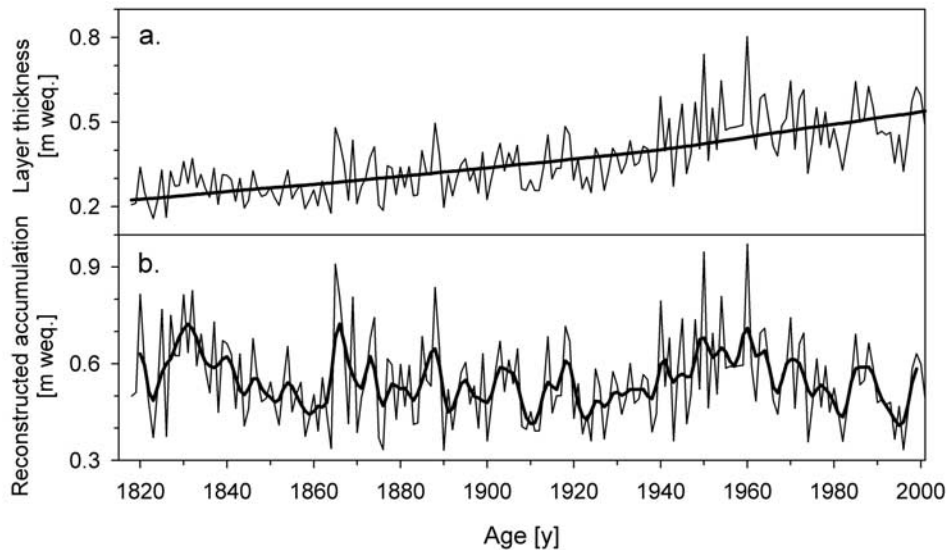


**Figure 2.** (a) Annual layer thickness profile for the Belukha ice core for the time period 1816–2001 (thin line), superimposed with the model layer thickness profile as determined by a simple thinning function (thick line). (b) Resultant time series of reconstructed annual accumulation (thin line), superimposed with the five-sample running mean (weights 1-3-4-3-1) (thick line).

Altai since the final stage of the Little Ice Age ( $\sim 1450$ – $1850$  A.D.) [Grove, 1988].

## 2. Methods

### 2.1. Ice Core Recovery and Dating

[6] In July 2001, three ice cores were extracted from the glaciated Belukha col ( $49^{\circ}48'26.3''N$ ,  $86^{\circ}34'42.8''E$ , 4062 m a.s.l.) and returned to the Paul Scherrer Institute in a frozen state [Olivier *et al.*, 2006]. Core 1 extended only to a depth of 27 m before a discontinuity in the core was recognized as evidence of a buried crevasse. Drilling was reestablished 22 m to the north, resulting in core 2 that reached a depth of 86 m before technical problems necessitated the introduction of ethylene glycol. A bedrock core was obtained within 3 m of this site to a depth of 140 m, though the top 50 m of this core 3 were necessarily left behind. The circumstantial core replication has the advantage of duplicate stratigraphic records over much of the last 200 years. Here, results of the analysis of the 86 m long core 2 are discussed, if not specified otherwise. An exception is the melt percent profile, which was also determined for core 1 and part of core 3. Most of the ice at the drilling sites was deposited along a 150 m upstream flowline starting at the bergschrund. The elevation difference is roughly 50 m so that a significant change in precipitation amount and composition is unlikely [Olivier *et al.*, 2003].

[7] The initial age scale of the Belukha core was derived from the 1963 peak in tritium and the  $^{210}\text{Pb}$  record, applying a nonlinear regression to account for the expected layer thinning in the lower part [Olivier *et al.*, 2004]. In addition, a three-parameter annual layer counting methodology was developed, using the high-resolution records of melt percent,  $\delta^{18}\text{O}$ , and ammonium concentration. As discussed by Olivier *et al.* [2006], this layer counting was found to be closely consistent with the initial age scale, when calibrated

with volcanic horizons detected in the excess sulfate record. The eruptions of Katmai, Alaska (1912) and Tambora, Indonesia (1815/1816) were identified at depths of 53.8 m (40.0 m weq.) and 86.6 m (69.5 m weq., in core 3), respectively. Positive corrections to the original uncalibrated counting of five and nine years were required to align the two volcanic horizons at 1912 and 1816, respectively. The resulting time period covered by the ice core is 1816–2001. The degree of uncertainty in the annual dating varies in connection to the proximity to the surface and the three reference horizons in 1963, 1912, and 1816. Within one decade of each horizon, the accuracy is estimated to be  $\pm 1$  year, but outside these ranges (1826–1902, 1922–1953, and 1973–1990) it rises to  $\pm 2$ – $3$  years. In the following, the layer-counted age scale is used for all data presentations.

[8] For identifying annual layer boundaries, local maxima of the three parameters were used. On average, the offset of annual layer boundaries derived from different parameters were minor. However, a small apparent shift was detectable in the position of the melt percent maxima, which on average were located at greater depths equivalent to  $\sim 9\%$  of the annual accumulation. This shift is expected since meltwater penetrates into deeper layers, but it also indicates that the penetration depth is limited over most of the last two centuries. A notable exception was the zone of very high melt in the top 10 m of the core, which revealed maxima in melt percent that were nearly opposite in phase to the geochemical parameters. This suggests a significantly higher degree of percolation during the most recent decade.

### 2.2. Accumulation Reconstruction

[9] Accumulation histories can be reconstructed from annual layer thickness profiles by means of glacier flow models to correct for the nonlinear thinning of layers with depth. The simple steady state model, which was already applied for dating, was used (Figure 2a). This model relies

on a representative surface accumulation estimate and a constant value for the vertical strain rate [Haefeli, 1961]. A basic model of this type [Nye, 1963; Dansgaard and Johnsen, 1969] proved adequate for the work presented herein, as thinning would become severe only in the lower reaches of the glacier, i.e., below that covered by the investigated ice core. Reconstructed accumulations (Figure 2b) were then determined from the ratio of the layer thickness of each year to the modeled thickness, multiplied by the surface accumulation rate. In addition, annual layer thicknesses were corrected for the moderate tilting of layers at depth. For that purpose a smooth parabolic function was fit to the layer tilt measurements below 20 m depth, the point at which the gradual tilting began. A maximum tilt of  $27.5^\circ$  was observed at the base of the ice core, producing a layer thickness bias of 11%.

### 2.3. Stable Oxygen Isotope ( $\delta^{18}\text{O}$ ) Analysis

[10] The analytical method used for  $\delta^{18}\text{O}$  analysis involved pyrolysis of melted ice samples at  $1450^\circ\text{C}$  in a glassy carbon reactor, to produce carbon monoxide (CO) [Gehre and Strauch, 2003; Kornxl et al., 1999]. The subsequent measurement of the relative proportions of  $^{12}\text{C}^{16}\text{O}$  and  $^{12}\text{C}^{18}\text{O}$  was done by standard isotope ratio-mass spectrometry (Delta Plus XL, Finnigan MAT).  $\delta^{18}\text{O}$  is defined as the per mil difference between the sample composition and the Standard Mean Ocean Water, SMOW. The precision of the measurements was  $\pm 0.2\%$ . Sampling intervals were identical to those used for ion analysis and ranged from 3 to 5 cm.

### 2.4. Ice Core Melt Percent

[11] High-resolution melt percent profiles were generated to fit the sampling interval (3–5 cm) as predetermined by the cutting process for ion analysis and  $\delta^{18}\text{O}$  determination. Melt features were generally of limited thickness, rarely more than 2 cm except for several large coherent melt zones in the top 10 m. Because of very cold ice temperatures at depth ( $-16.6^\circ\text{C}$  at 15 m [Olivier et al., 2003]), percolation activity has remained minimal until the most recent decade.

[12] Meltwater-infiltrated layers appear bright and bubble-free when the core is backlit in a darkened room, and were classified and quantified by visual evaluation. Such techniques have been demonstrated to yield reproducible melt percent profiles independent of observer or classification scheme [Kotlyakov et al., 2004]. Whereas fully consolidated (uniformly bright) ice layers were attributed 100% weight, those layers that were incompletely or imperfectly consolidated (so-called “icy layers”) were assigned a weighting of 80%. Zones of only limited meltwater infiltration, e.g., identified as “icy firn” intervals in the uppermost layers, were also recorded and were given a weight of 20% in the calculation of meltwater amounts. The final melt percent profile largely reflected the presence of major ice layers ( $>1$  cm), and so this weighting methodology according to visual categorization had limited influence. All features were recorded to a resolution of 1 mm and those layers that intersected only a portion of the 7.6 cm diameter core were weighted always by 50%. Wedge-shaped or otherwise irregular ice layers were measured on opposite sides of the core and

mean thicknesses were used. Vertical “pipe” features that act as conduits for percolating meltwater were of limited scale and only observed at shallow depths; such “chance” features were not considered part of the melt stratigraphy and were not quantified. At depths below 50 m, some intervals of the ice core were cracked to an extent that prevented accurate detection of layers. This resulted occasionally in data gaps of typically less than 20 cm, except for three larger disturbed zones of 50–60 cm thickness in core 3, precluding the determination of melt percentages for a total of five accumulation years. Within the firn section, melt percentages were calculated on an ice-equivalent basis, given that meltwater-ice layers do not undergo compressional densification.

[13] Cross-core matching with core 1 and core 3 was accomplished iteratively by first recognizing certain distinctive features in each core, and creating a temporary depth adjustment to align those features to their respective positions on the depth scale. For matching core 2 and core 3, a very prominent dust horizon at 75.6 m depth dated to 1842 was additionally used [Olivier et al., 2006]. The high-resolution melt percentages for cores 1 and 3 were then compared to core 2, at which point additional features and patterns were recognizable enabling further refinement to the depth rescaling. The inclination angle of ice layers was also registered throughout each core. Very similar profiles were found in cores 2 and 3 confirming that the internal layer tilting was a property of the glacier and not caused by nonvertical ice core drilling. The resulting annually averaged melt percent profiles are shown in Figure 3.

## 3. Calibration Methods

### 3.1. The $\delta^{18}\text{O}$ Temperature Calibration

[14] For the calibration of  $\delta^{18}\text{O}$  values as a paleothermometer real-time data generated for the IAEA Global Network of Isotopes in Precipitation (GNIP) were used [International Atomic Energy Agency/World Meteorological Organization (IAEA/WMO), 2004; Rozanski et al., 1993]. Monthly data for the single year 1990 were available from a total of nine stations in central Asia, between  $70\text{--}120^\circ\text{E}$  longitude and  $35\text{--}60^\circ\text{N}$  latitude. The sites included Enisejsk, Irkutsk, Novosibirsk, and Omsk in Russia, and Zhangye, Urumqi, Baotou, Shijiazhuang, and Tianjin in China, all located north of the monsoonal boundary that represents a reversal in the  $\delta^{18}\text{O}$ -surface air temperature ( $T_{\text{sfc}}$ ) relationship [Araguás-Araguás et al., 1998; Tian et al., 2001]. Additionally, data generated sporadically during the decade of the 1990s (primarily 1996–2000) from Ulan Bator, Mongolia, could be compiled to create an additional point [IAEA/WMO, 2004]. When plotting the March–November (the assumed precipitation season for Belukha, as indicated in section 4.2) average precipitation- $\delta^{18}\text{O}$  value at each station against the corresponding March–November averages of  $T_{\text{sfc}}$ , the relationship depicted in Figure 4 resulted. A linear regression of these data produced the paleothermometry equation,  $\delta^{18}\text{O} = (0.55 \pm 0.26) T_{\text{sfc}} - (16.9 \pm 3.2)\%$ , where the slope and intercept values have been defined as “ $\alpha$ ” and “ $\beta$ ,” respectively [Cuffey et al., 1995]. The uncertainty estimation is based on a 95% confidence interval ( $n = 10$ ). When considering paleodata interpreta-

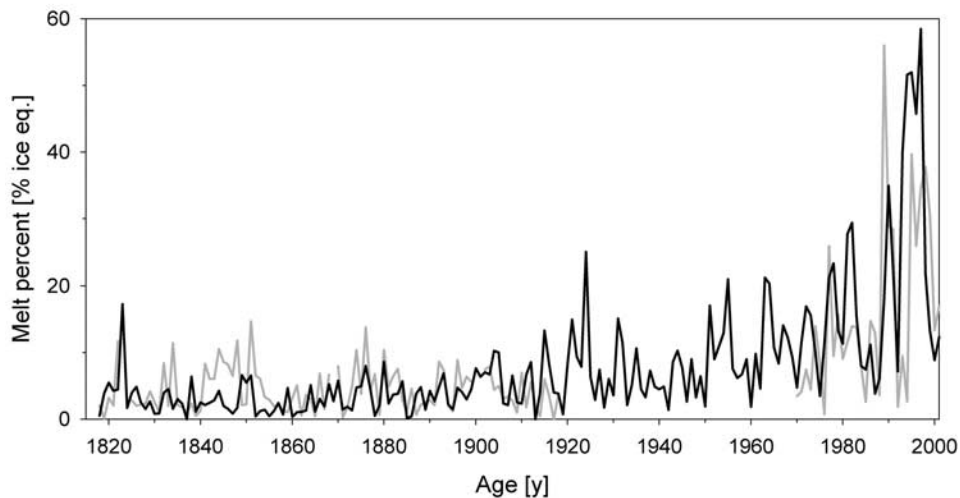


**Figure 3.** Annually averaged melt percent values for Belukha core 2 (thick, solid line) over the entire 1816–2001 period, plus the same for core 1 (1970–2001) and core 3 (1816–1918) (both thick, shaded lines).

tion at a single geographical point, the  $\beta$  value is less critical, whereas the slope parameter is paramount to properly assessing the magnitude of atmospheric temperature changes over time. Typical  $\alpha$  values in the range between 0.65 and 0.75‰/°C are common for present-day observations in high-latitude and polar regions [Paterson, 1994], whether determined by time series data from a single location, or alternately (as in Figure 4) by taking into account long-term averages from many locations.

[15] The calibration slope of 0.55‰/°C is consistent with results from other studies in high-elevation locations in central Asia, including the Tien Shan mountains ( $\delta^{18}\text{O} = 0.60T_{\text{sfc}} - 5.6\text{‰}$  [Aizen *et al.*, 1996]), as well as from a network of stations over much of northern Tibet ( $\delta^{18}\text{O} = 0.60T_{\text{sfc}} - 12\text{‰}$  [Yao and Thompson, 1992; Lin *et al.*, 1995]). For this reason, the  $\alpha$  value of  $0.55 \pm 0.26\text{‰}/\text{°C}$  was deemed appropriate for the determination of temperature anomalies from the annually averaged  $\delta^{18}\text{O}$  time series from the Belukha core.

### 3.2. Application of Melt Percent as a Summer Temperature Proxy

[16] In glaciated regions where surface melting in summer is present, the temporal changes in melt percentages have been successfully applied as summer temperature proxy records [Koerner and Fisher, 1990; Kotlyakov *et al.*, 1990; Kameda *et al.*, 1995; Grumet *et al.*, 2001]. Tarussov [1992] used the following empirical formula, based on data from the Eurasian Arctic, relating the quantity of meltwater ( $A$ , mm) formed during any given summer to the mean June–August temperature ( $T_{\text{JJA}}$ , °C) at the snow surface:

$$A = (T_{\text{JJA}} + 9.5)^3$$

[17] The measured melt percent provides a direct determination of the parameter  $A$ . Since melt layers themselves form within firn layers that initially contain approximately

50% pore volume (density  $\sim 0.45 \text{ g/cm}^3$ ), the total annual meltwater formation can be given as:

$$A = 0.50 M * b$$

where  $M$  is the annually averaged melt percent (on an ice-equivalent basis), and  $b$  is the reconstructed accumulation (mm weq.) for that same year. Whereas the original formula [Tarussov, 1992] made the assumption of wetted firn grains (representing 0.09, or 18% of the original pore volume), a condition likely for low-lying Arctic island glaciers, the formula here is altered to remove that assumption. Instead,

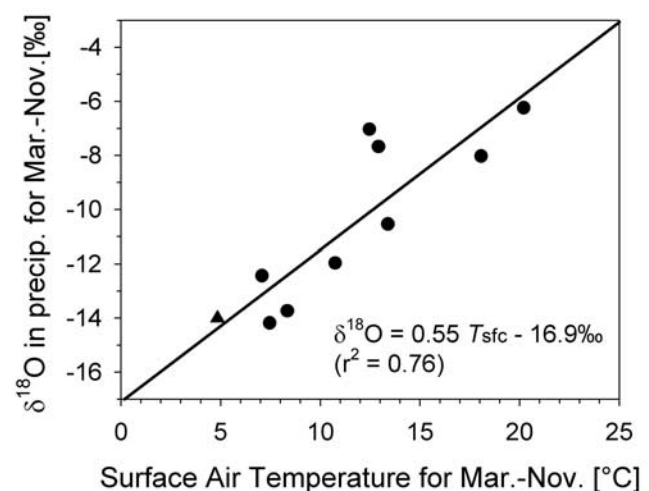


**Figure 4.** Linear relationship between surface air temperature ( $T_{\text{sfc}}$ ) and  $\delta^{18}\text{O}$  in precipitation (both March–November averages) at nine GNIP stations in central Asia (35–60°N, 70–120°E) for the year 1990 (see text), except for the longer-term averages at Ulan Bator, Mongolia (triangle).

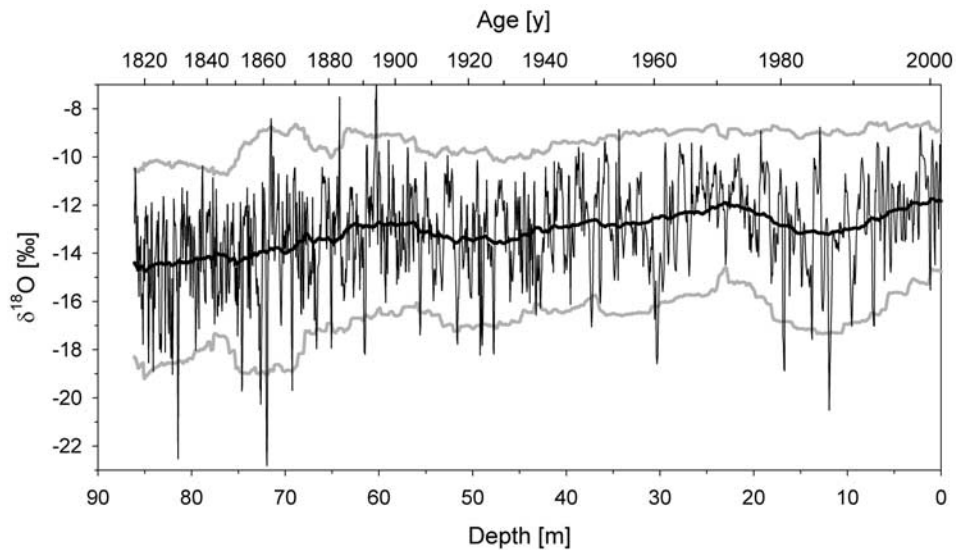


**Figure 5.** The  $\delta^{18}\text{O}$  profile from the Belukha ice core for the time period 1816–2001 (thin line), superimposed with the 199-sample running mean (thick, solid line) and the area bounded by this line  $\pm 2\sigma$  (thick, shaded lines).

“icy firn” layers were included in the calculations of  $M$  (see section 2.4). The average summer temperatures for Belukha glacier then were estimated from the melt percent record by:

$$T_{\text{JJA}} = (0.50 M * b)^{1/3} - 9.5$$

[18] Because of the strong cubic-root function, the proxy capability of melt paleothermometry is somewhat limited. Given possible amounts of accumulation in most areas of the world, average summer temperatures above  $0^\circ\text{C}$  would almost certainly yield 100% melt infiltration, or so-called “superimposed” ice. Of course, such a condition would not yield any temporal record in melt percent, so the effective range as applied to Belukha glacier is more accurately  $-3.5^\circ\text{C}$  ( $\sim 85\%$  melt) and below. Naturally, a lower limit to the proxy capability also exists in the case of unusually cold summers, when melt layers are no longer formed (0% melt,  $T_{\text{JJA}} \leq -9.5^\circ\text{C}$ ). In generally colder times, a higher relative contribution from thin ice layers ( $< 3$  mm), i.e., those which may have resulted primarily from radiative or wind effects, is likely and complicates the nature of the melt percent- $T_{\text{JJA}}$  relationship. Stemming from the strongly non-linear function of the melt percent- $T_{\text{JJA}}$  relationship, only minor differences in absolute percentages can translate into large variations of  $T_{\text{JJA}}$  when melt occurrence is low ( $\leq 5\%$ ). Hence, in case of Belukha glacier the melt paleothermometry is fully applicable only in the temperature range from  $-7.2^\circ\text{C}$  to  $-3.5^\circ\text{C}$  ( $5\% \leq M \leq 85\%$ ).

## 4. Results and Discussion

### 4.1. Temporal Variation of Accumulation

[19] The profile of reconstructed annual accumulation from Belukha ice core (Figure 2b) shows only moderate variability and no trend over the past two centuries. However, one should note that because accumulation reconstructions are dependent upon the age-depth scale in terms of

both magnitude and timing, the finer detail of this time series is more susceptible to occasional errors in layer counting than the intrinsic core parameters. Two minor maxima centered around 1830 and 1950 are observed. The latter event appears also in the 60-year precipitation history from the nearby high-elevation station Kara-Tyurek ( $49^\circ 59'\text{N}$ ,  $86^\circ 14'\text{E}$ , 2600 m a.s.l.,  $\sim 30$  km northwest of Belukha), although the trends over the past three decades are not similar between the two. Nevertheless, both the absolute amount of precipitation and the scale of variability are quite similar over the period of overlap (1939–2000), with  $0.56 \pm 0.15$  ( $1\sigma$ ) m weq./y for Belukha glacier and  $0.59 \pm 0.08$  ( $1\sigma$ ) for Kara-Tyurek. A comparable precipitation amount of  $0.55 \pm 0.07$  ( $1\sigma$ ) was reported at nearby Ak-kem station ( $49^\circ 58'\text{N}$ ,  $86^\circ 42'\text{E}$ , 2000 m a.s.l.,  $\sim 10$  km north of Belukha) for the time period 1968–2000).

### 4.2. The $\delta^{18}\text{O}$ Temperature History From the Belukha Ice Core

[20] The complete  $\delta^{18}\text{O}$  profile (Figure 5) is characterized by consistent high-frequency variance reflecting seasonal variations in temperature. In addition, a gradual upward trend toward the present is observed. However, the record is also punctuated with a number of sharply deviating events of limited duration. Most of these events show more negative  $\delta^{18}\text{O}$  values than the corresponding 199-sample running mean minus two standard deviations, resulting in a moderate skewness of  $-0.60$  in the distribution of anomaly values.

[21] The Belukha  $\delta^{18}\text{O}$  record is considered as representative of spring, summer, and autumn temperatures, because precipitation data from nearby Ak-kem station show a strong seasonal distribution (Figure 6). Summer months (June–August) contribute 58% of the total precipitation, while winter months (December–February) account only for 4%. This suggests that very negative  $\delta^{18}\text{O}$  values represent those rare occasions when significant snowfalls occurred in midwinter months on Belukha glacier. These

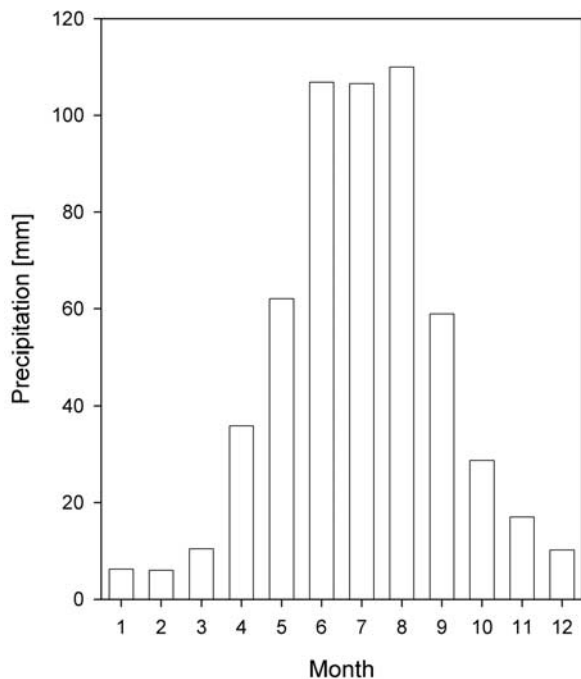


**Figure 6.** Annual distribution of the precipitation in Ak-kem (2000 m a.s.l., ~10 km north of Belukha) averaged over the time period 1990–2000.

anomalously low values would therefore leave false signatures in the temperature proxy record. To reduce such a bias, all those points more negative than the corresponding 199-sample running mean minus two standard deviations were removed. This process eliminated just 2.7% of the values, reduced the skewness coefficient to  $-0.10$ , and in the end had virtually no influence on the large-scale trends discussed in later sections. All future discussion of this data series was undertaken on the basis of a March–November accumulation year. From now on the word annual means is used for the average over an annual accumulation layer, which is assumed to represent March–November.

[22] The annually averaged  $\delta^{18}\text{O}$  values are depicted in Figure 7a, along with a smoothed version of the curve to highlight interdecadal trends. Applying the value of  $0.55 \pm 0.26\text{‰}/^\circ\text{C}$  as the  $\alpha$ -coefficient as discussed in section 3.1, resulted in the temperature anomaly scale included on the right-hand side. Here, the zero value is set to match the average  $\delta^{18}\text{O}$  value for the entire record of  $-13.1\text{‰}$ . In general, the profile shows an initial 40-year period of persistent cold temperatures through the mid-19th century, ending with an abrupt transition at  $\sim 1860$  to warmer conditions. This is then followed by a more gradual warming trend until the present, superimposed with decadal-scale fluctuations. Assuming a linear trend since the late cold phase of the local LIA in the mid-19th century, the  $\delta^{18}\text{O}$  paleothermometry would suggest a sustained warming of  $2.5 \pm 1.7^\circ\text{C}$  over the last 150 years in this region. The uncertainty is calculated by error propagation from the uncertainty of the linear regression slope  $b$  of  $\delta^{18}\text{O}$  versus time ( $b = 0.0093 \pm 0.0043\text{‰}/\text{year}$ , 95% confidence interval,  $n = 152$ ) and from the uncertainty of the  $\alpha$ -coefficient ( $\alpha = 0.55 \pm 0.26\text{‰}/^\circ\text{C}$ , 95% confidence interval,  $n = 10$ ).

### 4.3. Melt-Inferred Temperature History From the Belukha Cores

[23] The summer season temperatures, as determined from the melt percent and accumulation histories, is depicted in Figure 7b. The annual averages were calculated using all data, including those from the other two partial cores. With the incorporation of core 1 and 3 melt percent profiles, nearly 70% of the 184 years melt history consists of averages over two cores, producing a record that better accounts for lateral inhomogeneity. The melt-inferred  $T_{\text{JJA}}$  series suggest very little warming before the onset of the 20th century, but as  $T_{\text{JJA}}$  values are mainly below  $-7.2^\circ\text{C}$ , they lie outside the melt percent sensitivity range at Belukha glacier ( $-7.2^\circ\text{C}$  to  $-3.5^\circ\text{C}$ , section 3.2). Hence melt-inferred  $T_{\text{JJA}}$  estimates below  $-7.2^\circ\text{C}$  can only be considered as upper limits of the summer temperature. Consequently, an interpretation of the full magnitude of the warming trend from melt-inferred  $T_{\text{JJA}}$  estimates is possible only over the last century. For that time period  $T_{\text{JJA}}$  estimates suggest a persistent warming trend that is approximately linear, and is superimposed on a strong interannual variability. A simple linear regression of these data yields a warming of  $1.6 \pm 0.4^\circ\text{C}$  over the 20th century (95% confidence interval) compared to a  $\delta^{18}\text{O}$ -inferred  $1.7 \pm 1.1^\circ\text{C}$  -warming over the same time period.

[24] Evidence of a recent onset of multiannual meltwater percolation is provided by the comparison of core 1 and 2 melt percent profiles (Figure 3), where sequences of strong summer melt over several years terminate at different points in the respective cores. In the first instance, propagating meltwater seemed to reach a depth corresponding to summer 1993 in core 2, forming a pair of major ice layers of  $\sim 5$  cm and  $\sim 11$  cm thickness. In contrast, core 1 revealed only a 1.2 cm thick ice layer, and correspondingly low annual melt percent. In the subsequent high-melt zone the situation was reversed, with a  $\sim 5$  cm thick ice layer corresponding to the summer 1988 for core 2 and a  $\sim 19$  cm thick layer for the same year in core 1. Such intercore variability may have been possible simply by the lateral inhomogeneity true for any glacier. However, the observed sequence of ice layers with depth suggests vertical movement within successive years. On the basis of data from nearby meteorological stations and representative lapse rates ( $\sim 0.65^\circ\text{C}/100$  m), average temperatures in summer months at the elevation of Belukha glacier currently range between  $-4^\circ\text{C}$  (June) and  $0^\circ\text{C}$  (July), thus allowing for persistent melting.

[25] Finally, a strong synchronicity between very cold summers in the Belukha melt-inferred  $T_{\text{JJA}}$  record and large volcanic eruptions was recognized. Four of the most extreme  $T_{\text{JJA}}$  events (indicated by diamonds in Figure 7b) appear coincident with the accumulation years starting in the years following the eruptions of Coseguina (1836–1837), Krakatau (1884–1885), Katmai (1912–1913), and Pinatubo (1991–1992). These events were all recorded by low-melt occurrence in both of a pair of Belukha ice cores (Figure 3), such that random anomalies due to spatial inhomogeneity are unlikely. However, one has to keep in mind that for the first three events, the melt-inferred  $T_{\text{JJA}}$  represent only upper limits, as detailed in section 3.2.

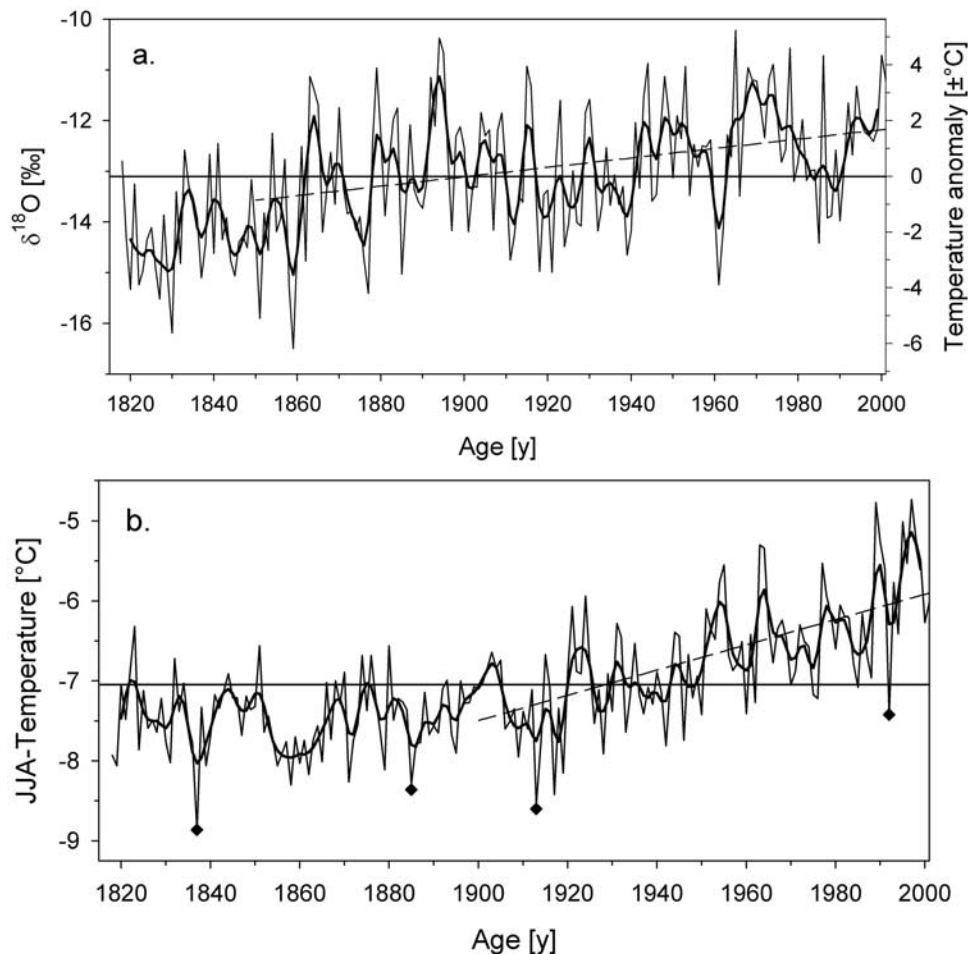


**Figure 7.** (a) Time series of March–November  $\delta^{18}\text{O}$  averages from the Belukha ice core (thin line) superimposed with the five-sample moving average (weights 1-3-4-3-1; thick line), the right-hand axis representing the temperature anomaly scale based on a  $\delta^{18}\text{O}$ - $T_{\text{sfc}}$  slope of  $0.55\text{‰}/^\circ\text{C}$ . The zero value is set to match the average  $\delta^{18}\text{O}$  value for the entire record of  $-13.1\text{‰}$ . The dashed line indicates the warming trend of  $\sim 2.5^\circ\text{C}$  over the last 150 years. (b) Average  $T_{\text{JJA}}$  estimates from Belukha melt percent records (thin line) and the five-sample moving average (weights 1-3-4-3-1; thick line). Annual melt percent averages were calculated using all data, including those from the other two partial cores. The dashed line indicates the warming trend of  $\sim 1.6^\circ\text{C}$  over the last 100 years. The diamonds indicate years following four major northern hemisphere volcanic eruptions (see text).

#### 4.4. Comparison With Instrumental Data and Other Archives

[26] Instrumental temperature data from Barnaul, Russia ( $52^\circ 26'\text{N}$ ,  $83^\circ 31'\text{E}$ , 184 m a.s.l., 360 km northwest of Belukha) covering the period 1851–1999 were obtained from Global Historical Climatology Network (GHCN) version 2 [Vose *et al.*, 1992; Peterson and Easterling, 1994]. Instrumental records of this length have necessarily been assembled from data collected under varying circumstances, as procedures have changed over the years and monitoring stations have been moved. Specifically for Barnaul, the nonhomogenized 150-year GHCNv.2 time series was apparently derived from five separate data segments, requiring discontinuity adjustments of up to  $1.3^\circ\text{C}$  in order to produce a single coherent time series [Vose *et al.*, 1992]. In Figure 8, the two independent temperature reconstructions ( $T_{\text{JJA}}$  and  $T_{\text{March–Nov}}$ ) from the Belukha ice cores are shown, overlaid in each case with the corresponding

temperature time series from Barnaul. The respective  $T_{\text{JJA}}$  time series clearly share strong similarities (Figure 8a), especially among the interannual variations during the 20th century. However, the magnitude of the warming trend is much less pronounced for the Barnaul temperatures, which show only a  $0.78^\circ\text{C}$  linear rise from 1900 to 1999, to compare to the  $1.6^\circ\text{C}$  change inferred from the Belukha melt percent.

[27] The  $T_{\text{March–Nov}}$  time series from  $\delta^{18}\text{O}$  paleothermometry and the Barnaul temperature record both reveal an equally strong warming trend over the last 150 years of  $2.5^\circ\text{C}$  and  $2.4^\circ\text{C}$ , respectively (Figure 8b). However, only moderate similarities are observed at the subdecadal scale. The larger variations in the  $\delta^{18}\text{O}$ -inferred  $T_{\text{March–Nov}}$  likely represent precipitation bias, or perhaps postdepositional alteration. In certain cases (e.g.,  $\sim 1940$  and  $\sim 1960$ ), prominent minima in the  $\delta^{18}\text{O}$ -inferred  $T_{\text{March–Nov}}$  appear coincident with similar minima in the historical temperatures,

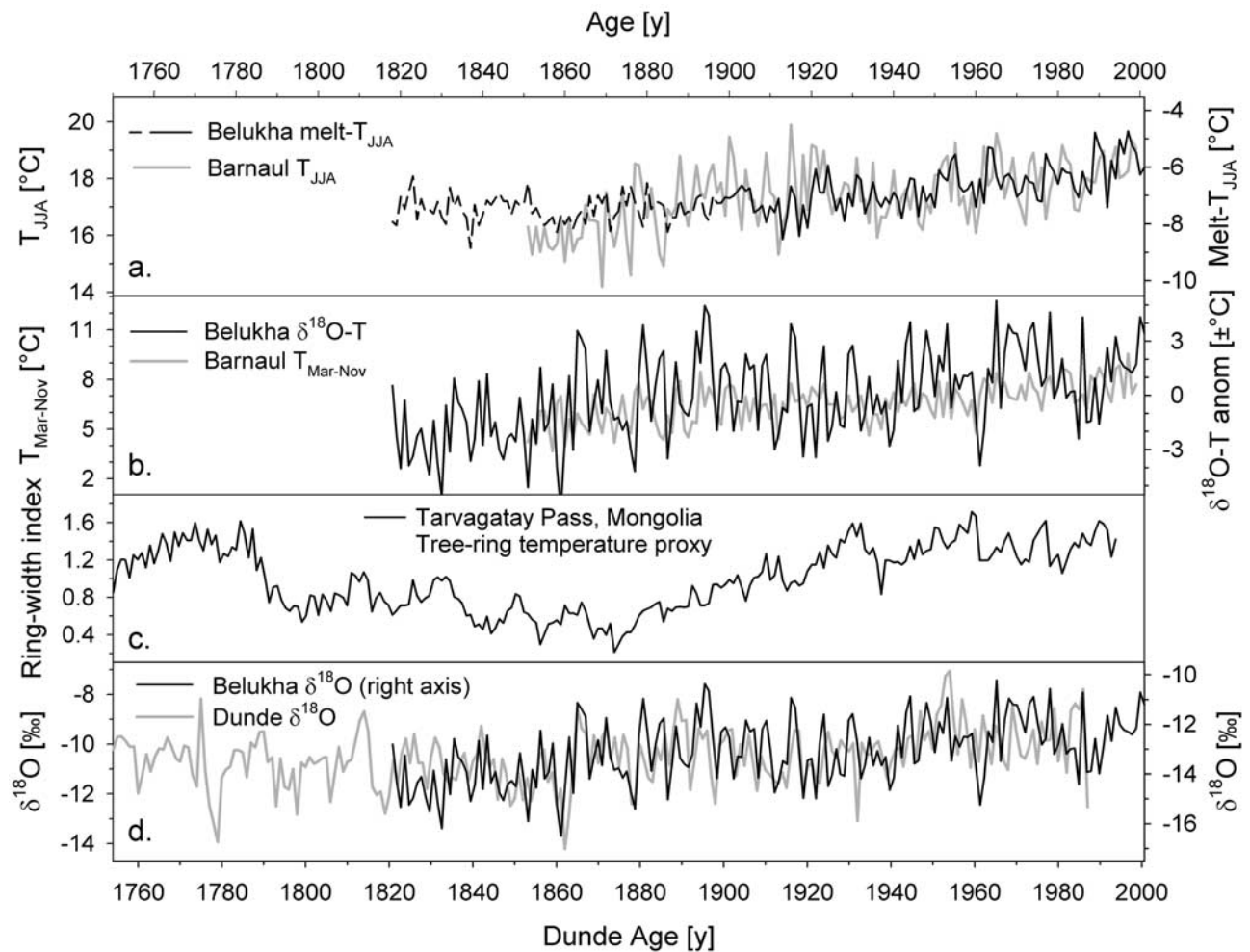


**Figure 8.** (a) Comparison of the annual melt-inferred  $T_{JJA}$  averages from the Belukha glacier (solid line, dashed line for the period 1816–1900, for which the melt-inferred  $T_{JJA}$  gives only an upper limit of the temperature, see text) with the summer (JJA) averages of air temperature at Barnaul (shaded line). (b) Comparison of annual  $\delta^{18}\text{O}$  inferred temperature anomalies from the Belukha ice core (solid line) with the March–November averages of air temperature at Barnaul, Russia (shaded line). (c) Temperature-sensitive ring width index from Tarvagatay Pass, Mongolia ( $48^{\circ}18'N$ ,  $98^{\circ}56'E$ , 2420 m a.s.l.) [*Jacoby et al.*, 1996]. (d) Comparison of  $\delta^{18}\text{O}$  annual averages from the Belukha ice core (solid line) and from Dunde ice core, China ( $38^{\circ}06'N$ ,  $96^{\circ}24'E$ , 5325 m a.s.l.; shaded line, timescale aligned to improve match).

though the variations in the latter are almost always of lower magnitude. Hence exaggerations of the fluctuations in the Altai environment appear to have been imprinted on the ice core  $\delta^{18}\text{O}$  profile by factors other than temperature. The very strong seasonality in the accumulation at Belukha implies the possibility of biases in the temporal profile of  $\delta^{18}\text{O}$  as a function of a nonconstant seasonal snowfall distribution. This is almost certainly one of the causes for the large degree of variance in the record.

[28] Through comparison with the temperature-sensitive tree ring history from Tarvagatay Pass, Mongolia ( $48^{\circ}18'N$ ,  $98^{\circ}56'E$ , 2420 m a.s.l., for location see Figure 1, 915 km east-southeast of Belukha, Figure 8c, [*Jacoby et al.*, 1996]) one can assume that  $\delta^{18}\text{O}$ -inferred temperatures in the lowest ice core section represent a late-LIA minimum level. The absolute magnitude of temperature change for west-central Mongolia was not explicitly determined, although

the authors noted a strong relationship between their tree ring history and the large-scale warming detailed in historical and proxy compilation records for the Northern Hemisphere and Arctic. Whether temperature variations between the two locations should be expected to have close coherence remains unclear. This is true especially because of the sizable distance and dissimilar settings between the sites, the tree ring history coming from a north facing slope on the northeast margin of the Hungai mountains. Specifically, whereas both proxy records indicate a steady post-LIA temperature rise, there appears to be a lag in the tree ring history as compared to the Belukha- $\delta^{18}\text{O}$  record. This suggests a possible time transgressive termination of the LIA, propagating eastward from the western Altai.

[29] In contrast, no significant temporal offsets between the post-LIA changes are apparent via a comparison of the high-resolution  $\delta^{18}\text{O}$  profiles from Belukha and another

central Asia ice core, from Dundu in the Qilian Shan, China (38°06'N, 96°24'E, 5325 m a.s.l., for location see Figure 1, 1500 km southeast of Belukha, Figure 8d [Davis and Thompson, 2004]). The two  $\delta^{18}\text{O}$  records were aligned through shifting the Dundu record by three years at 1817, which is in the range of uncertainty of the Dundu age-depth scale, generated without being restrained by horizon identification. Both  $\delta^{18}\text{O}$  records show similarities in the fine-scale behavior as well as comparable transitions at 1860 and 1940–1950. In addition, the overall magnitude of LIA-20th century warming at Dundu of 2.5°C (with  $\alpha = 0.55\text{‰}/^\circ\text{C}$ ) is in the same range as for the Belukha and Barnaul records. Finally, the behavior of the Dundu  $\delta^{18}\text{O}$  during the mid-18th century also differs significantly from the tree ring paleotemperature record from Mongolia. The closer agreement between the Belukha and Dundu  $\delta^{18}\text{O}$  records as compared to that with the tree ring history from Mongolia, despite the even larger geographical separation (1500 vs. 915 km), suggests that the mechanism of signal archiving (ice core vs. tree ring) has an important influence here in central Asia.

## 5. Conclusions

[30] The two Belukha ice core temperature proxies taken together indicate a strong warming trend in the order of  $1.6 \pm 0.4^\circ\text{C}$  during the summer month (JJA) and  $1.7 \pm 1.1^\circ\text{C}$  during March–November over the last century, inferred from melt percentages and the  $\delta^{18}\text{O}$  record, respectively. Assuming a linear trend since the late cold phase of the local LIA in the mid-19th century, the  $\delta^{18}\text{O}$  paleothermometry would suggest a sustained warming of  $2.5 \pm 1.7^\circ\text{C}$  over the last 150 years in this region. This represents a much larger warming than that suggested by most other paleoclimatic histories, including compilation products that represent hemispheric-scale variability [Esper et al., 2002; Mann and Bradley, 1999].

[31] More specifically, the ability to capture short-term summer temperature variability is stronger in the melt-inferred than in the  $\delta^{18}\text{O}$  proxy at Belukha, where precipitation seasonality is so extreme. However, the limited sensitivity of the melt index ( $-3.5$  to  $-7.2^\circ\text{C}$ ) effectively restricts the application of this paleothermometer to the most recent century. Also, because of brittle ice conditions at depth in Belukha glacier, which unfortunately caused a much higher rate of fracturing in the ice core, a quantifiable melt stratigraphy will not be possible at depth below 110 m. Therefore the early temperature history of the Belukha ice core record will necessarily be limited to the  $\delta^{18}\text{O}$  paleothermometry. There remains high confidence that century-scale variations in  $\delta^{18}\text{O}$  over the more distant past will be reflected in a quantifiable way, which is supported by the strong similarity between the respective  $\delta^{18}\text{O}$  histories from Belukha and Dundu, China, indicating that the glaciers at both sites are archiving large-scale variability.

[32] The recent occurrence of thick melt layers ( $>10$  cm), unprecedented in at least the past two centuries, indicates a change from the recrystallization to the cold-infiltration zone [Shumskii, 1964] for this high-elevation region of the Belukha glacier. Whereas the cold englacial temperatures (approximately  $-17^\circ\text{C}$ ) and low melt incidence observed over the bulk of the ice core satisfies the classification of recrystallization zone according to the Shumskii [1964]

nomenclature, it is clear that seasonal meltwater formation and percolation are rapidly accelerating. The sudden appearance of multiannual percolation is newly realized at Belukha glacier and gives notice that the conservative nature of accumulation and geochemical properties, including those providing temperature proxies, is currently under threat.

[33] **Acknowledgments.** We would like to thank Patrick Ginot and Beat Rufibach for drilling; Martin Lüthi, Henrik Rhyn, Dimitrii N. Kozlov, Sergej Derewitschikow, Vladimir Vashenzev, Andrej Jerjomin, Veronica Morozova, Alexander Chebotkin, and Igor Karakulko for their help during the expedition; and Christoph Kull for providing the automatic weather station. We also acknowledge Stella Eyrikh for the translation of many Russian documents, Matthias Saurer for his expertise in isotope ratio-mass spectrometry, Bert DeSmedt for providing the GHCN ver.2 Barnaul temperature record, Martin Lüthi for advice in glacier flow modeling, and Lonnie Thompson for providing the annual Dundu  $\delta^{18}\text{O}$  record.

## References

- Aizen, V., E. Aizen, J. Melack, and T. Martma (1996), Isotopic measurements of precipitation on central Asian glaciers (southeastern Tibet, northern Himalayas, central Tien Shan), *J. Geophys. Res.*, **101**(D4), 9185–9196.
- Araguás-Araguás, L., K. Froehlich, and K. Rozanski (1998), Stable isotope composition of precipitation over southeast Asia, *J. Geophys. Res.*, **103**(D22), 28,721–28,742.
- Cecil, L. D., J. R. Green, and L. G. Thompson (2004), *Earth Paleoenvironments: Records Preserved in Mid- and Low-latitude Glaciers*, 250 pp., Springer, New York.
- Cuffey, K. M., G. D. Clow, R. B. Alley, M. Stuiver, E. D. Waddington, and R. W. Saltus (1995), Large Arctic temperature change at the Wisconsin-Holocene glacial transition, *Science*, **270**, 455–458.
- Dansgaard, W., and S. J. Johnsen (1969), A flow model and a time scale for the ice core from Camp Century, Greenland, *J. Glaciol.*, **8**, 215–223.
- Davis, M. E., and L. G. Thompson (2004), Four centuries of climatic variations across the Tibetan Plateau, in *Earth Paleoenvironments: Records Preserved in Mid- and Low-latitude Glaciers*, edited by L. D. Cecil, J. R. Green, and L. G. Thompson, pp. 145–161, Springer, New York.
- Dyurgerov, M. B., and M. F. Meier (2000), Twentieth century climate change: Evidence from small glaciers, *Proc. Natl. Acad. Sci. U. S. A.*, **97**, 1406–1411.
- Esper, J., E. R. Cook, and F. H. Schweingruber (2002), Low-frequency signals in long tree-ring chronologies for reconstructing past temperature variability, *Science*, **295**, 2250–2253.
- Gehre, M., and G. Strauch (2003), High-temperature elemental analysis and pyrolysis techniques for stable isotope analysis, *Rapid Commun. Mass Spectrom.*, **17**, 1497–1503.
- Grove, J. M. (1988), *The Little Ice Age*, 524 pp., Methuen, New York.
- Grumet, N. S., C. P. Wake, P. A. Mayewski, G. A. Zielinski, S. J. Whitlow, R. M. Koerner, D. A. Fisher, and J. M. Woollett (2001), Variability of sea-ice extent in Baffin Bay over the last millennium, *Clim. Change*, **49**, 129–145.
- Haefeli, R. (1961), Contribution to the movement and the form of ice sheets in the Arctic and Antarctic, *J. Glaciol.*, **3**(30), 1133–1151.
- International Atomic Energy Agency/World Meteorological Organization (2004), Global Network of Isotopes in Precipitation, The GNIP Database, <http://isohis.iaea.org>, Vienna.
- Jacoby, G. C., R. D. D'Arrigo, and T. Davaajamts (1996), Mongolian tree rings and 20th-century warming, *Science*, **273**, 771–773.
- Jouzel, J., F. Vimeux, N. Caillon, G. Delaygue, G. Hoffman, V. Masson-Delmotte, and F. Parrenin (2003), Magnitude of the isotope/temperature scaling for interpretation of central Antarctic ice cores, *J. Geophys. Res.*, **108**(D12), 4361, doi:10.1029/2002JD002677.
- Kameda, T., H. Narita, H. Shoji, F. Nishio, Y. Fujii, and O. Watanabe (1995), Melt features in ice cores from Site J, southern Greenland: Some implications for summer climate since 1550, *Ann. Glaciol.*, **21**, 51–58.
- Klinge, M., J. Böhner, and F. Lehmkuhl (2003), Climate pattern, snow- and timberlines in the Altai mountains, central Asia, *Erdkunde*, **57**, 296–308.
- Koerner, R. M., and D. A. Fisher (1990), A record of Holocene summer climate from a Canadian high-Arctic ice core, *Nature*, **343**, 630–631.
- Kornel, B. E., M. Gehre, R. Hofling, and R. A. Werner (1999), On-line delta O-18 measurement of organic and inorganic substances, *Rapid Commun. Mass Spectrom.*, **13**, 1685–1693.
- Kotlyakov, V. M., V. I. Zagorodnov, and V. I. Nikolaev (1990), Drilling on ice caps in the Soviet Arctic and on Svalbard and prospects of ice core

- treatment, in *Arctic Research: Advances and Prospects, Part 2*, edited by V. M. Kotlyakov and V. Y. Sokolov, pp. 5–18, Nauka, Moscow.
- Kotlyakov, V. M., S. M. Arkhipov, K. A. Henderson, and O. V. Nagornov (2004), Deep drilling of glaciers in Eurasian Arctic as a source of paleoclimatic records, *Quat. Sci. Rev.*, *23*, 1371–1390.
- Lin, P. N., L. G. Thompson, M. E. Davis, and E. Mosley-Thompson (1995), 1000 years of climatic change in China: Ice core  $\delta^{18}\text{O}$  evidence, *Ann. Glaciol.*, *21*, 189–195.
- Lydolph, P. E. (1977), Eastern Siberia, in *Climates of the Soviet Union, World Survey of Climatology*, vol. 7, chap. 4, pp. 91–115, Elsevier, New York.
- Mann, M. E., and R. S. Bradley (1999), Northern Hemisphere temperatures during the past six millennium: Inferences, uncertainties, and limitations, *Geophys. Res. Lett.*, *26*(6), 759–762.
- Nye, J. F. (1963), Correction factor for accumulation measured by the thickness of the annual layers in an ice sheet, *J. Glaciol.*, *4*, 785–788.
- Olivier, S., et al. (2003), Glaciochemical investigation of an ice core from Belukha glacier, Siberian Altai, *Geophys. Res. Lett.*, *30*(19), 2019, doi:10.1029/2003GL018290.
- Olivier, S., S. Bajo, L. K. Fifield, H. W. Gäggeler, T. Papina, P. H. Santschi, U. Schotterer, M. Schwikowski, and L. Wacker (2004), Plutonium from global fallout recorded in an ice core from the Belukha Glacier, Siberian Altai, *Environ. Sci. Technol.*, *38*, 6507–6512.
- Olivier, S., C. Blaser, S. Brüttsch, H. W. Gäggeler, K. Henderson, A. Palmer, T. Papina, and M. Schwikowski (2006), Temporal variations of mineral dust, biogenic tracers, and anthropogenic species during the past two centuries from Belukha ice core, Siberian Altai, *J. Geophys. Res.*, doi:10.1029/2005JD005830, in press.
- Paterson, W. S. B. (1994), *The Physics of Glaciers*, 3rd ed., 480 pp., Elsevier, New York.
- Pattyn, F., B. DeSmedt, S. DeBrabander, W. Van Huele, A. Agatova, A. Mistrukov, and H. Declerq (2003), Ice dynamics and basal properties of Sofiyskiy Glacier, Altai Mountains, Russia based on DGPS and radio-echo sounding surveys, *Ann. Glaciol.*, *37*, 286–292.
- Peterson, T. C., and D. R. Easterling (1994), Creation of homogeneous composite climatological reference series, *Int. J. Climatol.*, *14*, 671–679.
- Rozanski, K., L. Araguás-Araguás, and R. Gonfiantini (1993), Isotope patterns in modern global precipitation, in *Climate Change in Continental Isotopic Records, Geophys. Monogr. Ser.*, vol. 78, pp. 1–36, AGU, Washington, D. C.
- Shumskii, P. A. (1964), *Principles of Structural Glaciology*, translated by D. Kraus, 497 pp., Dover, Mineola, N. Y.
- Tarussov, A. (1992), The Arctic from Svalbard to Severnaya Zemlya: Climatic reconstructions from ice cores, in *Climate Since 1500 A.D.*, edited by R. S. Bradley and P. D. Jones, pp. 505–516, Routledge, Boca Raton, Fla.
- Tian, L., V. Masson-Delmotte, M. Stievenard, T. Yao, and J. Jouzel (2001), Tibetan Plateau summer monsoon northward extent revealed by measurements of water stable isotopes, *J. Geophys. Res.*, *106*(D22), 28,081–28,088.
- Vose, R. S., R. L. Schmoyer, P. M. Steurer, T. C. Peterson, R. Heim, T. R. Karl, and J. K. Eischeid (1992), The Global Historical Climatology Network: Long-term monthly temperature, precipitation, sea level pressure, and station pressure data, *NDP-041*, Carbon Dioxide Inf. Anal. Cent., Oak Ridge Natl. Lab., Oak Ridge, Tenn.
- Wedeland, W. M., and R. A. Bryson (1981), Northern Hemisphere air-stream regions, *Mon. Weather Rev.*, *109*, 255–270.
- Yao, T., and L. G. Thompson (1992), Trends and features of climatic changes in the past 5000 years recorded by the Dunde ice core, *Ann. Glaciol.*, *16*, 21–24.

---

H. W. Gäggeler, K. Henderson, A. Laube, S. Olivier, and M. Schwikowski, Paul Scherrer Institute, CH-5232 Villigen PSI, Switzerland. (margit.schwikowski@psi.ch)

T. Papina, Institute for Water and Environmental Problems, 656099 Barnaul, Russia.